

SOUNDING ROCKET MEASUREMENTS OF THE SOLAR SOFT X-RAY IRRADIANCE

S. M. BAILEY¹, T. N. WOODS², L. R. CANFIELD³, R. KORDE⁴, C. A. BARTH²,
S. C. SOLOMON² and G. J. ROTTMAN²

¹*Center for Atmospheric Science, Hampton University Hampton, VA 23668, U.S.A.*

²*Laboratory for Atmospheric and Space Physics, University of Colorado, Boulder,
CO 80309-0590, U.S.A.*

³*National Institute of Standards and Technology, Physics Laboratory, Gaithersburg,
MD 20899-0001, U.S.A.*

⁴*International Radiation Detectors, 2527 West 237th Unit B, Torrance, CA 90505-5243, U.S.A.*

(Received 3 December, 1996; accepted 19 February, 1999)

Abstract. Measurements of the solar soft X-ray (XUV: 2 nm to 30 nm) irradiance were performed from a sounding rocket payload flown from White Sands Missile Range, New Mexico on 4 October 1993 and again on 3 November 1994. The soft X-ray instrumentation comprised of silicon photodiodes with thin films deposited directly onto their active areas. The deposited material and its thickness in conjunction with the sensitivity of an uncoated diode determine the passband and the sensitivity of these photometric devices. The measurements are interpreted in terms of appropriate SERF 1 (Hinteregger, Fukui, and Gilson, 1981) model solar spectra. It is found that the data are consistent with a solar spectrum that is on average approximately a factor of two times the model solar spectra. It is shown that the measured irradiances are in reasonable agreement with other experiments.

1. Introduction

The solar irradiance in the wavelength range below 30 nm is deposited mostly into the lower thermosphere at altitudes between 100 km and 150 km. This energy photoionizes the neutral constituents of the atmosphere and participates in the formation of the ionosphere. The photoelectrons created in this process interact further with the neutrals, leading to excitation, dissociation, and further ionization. Understanding these processes and their variability is hampered by the lack of solar irradiance measurements below 30 nm. Lean (1987) reviewed the history of solar irradiance measurements and the current understanding of the ultraviolet spectrum and its variability. The majority of knowledge on solar soft X-ray and EUV irradiance comes from Air Force measurements on the Atmospheric Explorer (AE) satellites and sounding rockets (Torr *et al.*, 1979; Hinteregger, Fukui, and Gilson, 1981; Torr and Torr, 1985). The AE measurements occurred during solar cycles 20 and 21. Reviews of other measurements of the solar soft X-ray irradiance can be found in Manson (1976), Feng, Ogawa, and Judge (1989), Kreplin and Horan (1992), and their references. These other measurements are sparse and therefore do not cover the full range of solar activity.



The limited amount of solar data made proxy models of the solar variability necessary. The first widely used model was that of Hinteregger, Fukui, and Gilson (1981). The proxies are the chromospheric H I $L\beta$ (102.6 nm) and the coronal Fe XVI (33.5 nm) emissions. As measurements of these emissions are not typically available, they are correlated with the Ottawa (or currently Penticon) 10.7 cm radio flux ($F_{10.7}$) and its 81 day average which have been available on a daily basis since 1947. The Hinteregger model is referred to as SERF 1 by the Solar Electromagnetic Radiation Flux subgroup of the World Ionosphere-Thermosphere Study.

Following the work of Hinteregger, Tobiska, and Barth (1990) developed a new model of the solar irradiance, named SERF 2. Lean (1990) compared the results of SERF 1 and SERF 2 over time scales of the 27 day solar rotation and the 11 year solar cycle and concluded that the two models predicted significantly different variability. Tobiska (1991) consequently revised the SERF 2 model. The new version was compared to SERF 1 and SERF 2 by Buonsanto, Solomon, and Tobiska (1992) who concluded that, at soft X-ray wavelengths, the Tobiska (1991) model produced more irradiance than SERF 1.

Atmospheric studies have also addressed the magnitude of the solar soft X-ray irradiances. Richards and Torr (1984, 1985) studied the consistency of photoelectron measurements and calculations using measured solar soft X-ray irradiances values. They found agreement in the calculated and observed ionospheric photoelectron fluxes if they scaled the solar irradiance below 25 nm by approximately a factor of two. Barth *et al.* (1988) and Siskind, Barth, and Cleary (1990) found that an assumed order of magnitude variability of solar soft X-rays in the wavelength range 2 nm to 5 nm reproduced the large changes in the nitric oxide density observed by sounding rockets and by the Solar Mesosphere Explorer (SME).

Previous work has demonstrated that the region of the solar spectrum responsible for most photoelectrons lies at and below 30.4 nm (Richards and Torr, 1984, 1985). The 30.4 nm emission comes from the solar chromosphere, whereas emissions shortward of 30.4 nm are from both the solar chromosphere and the solar corona. Chromospheric emission variability is better understood than coronal variability; chromospheric emissions at longer wavelengths have been observed more often and these emissions typically vary similarly over the solar cycle. Timothy and Timothy (1970) correlated the 30.4 nm irradiance measured by the OSO 4 spacecraft with both the Zurich sunspot number and the $F_{10.7}$ flux. Recently, Richards, Fennely, and Torr (1994a, b) developed a proxy model called EUVAC which increased the solar XUV irradiances by a factor of 2 to 3 as compared to the SERF 1 model.

Since the AE-E measurements, there has been little data to add to our understanding of the magnitude and the variability of the solar soft X-ray irradiance. The poor reflectivity of most materials in the soft X-ray region makes it difficult to use conventional grating spectrometers in this wavelength regime. Thus we have developed photometers as an alternative method. Photometry however requires the use of filters for wavelength selection. In the soft X-ray region, thin film foils are

often used as filters. The difficulty with foil filters lies in their tendency to develop pinholes that transmit the much brighter longer wavelength sunlight. Ogawa *et al.* (1990) measured the solar extreme ultraviolet (EUV) and soft X-ray irradiance from a sounding rocket using a photodiode with a thin aluminum coating as well as an aluminum foil filter. By subtracting a constant background from their data due to pinholes and other light leak problems, they were able to conclude that the measured current from the photodiode, most sensitive in the range 17 nm to 80 nm, was consistent with their other measurements of the solar irradiance from 5 nm to 50 nm with a helium ionization chamber. The experiment described here also uses photodiodes to measure solar soft X-ray irradiance. For this work there are no foils; all filter materials are deposited directly on the photodiode. The following sections describe the development of these soft X-ray photometers along with their data and results from two rocket flights.

2. Experiment

The rocket experiment carried a host of instrumentation for the measurement of the solar irradiance. The spectral coverage ranged from 0.01 nm to 121.6 nm with varying resolution. The instruments and the payload are described by Woods *et al.* (1994). The solar instruments include an EUV grating spectrograph for measuring solar irradiance from 25 nm to 110 nm at 0.3 nm resolution (Woods and Rottman, 1990) as well as two dimensional imagers for imaging the solar atmosphere at EUV and soft X-ray wavelengths. Also on board was an airglow spectrograph which measured the terrestrial emissions in the far ultraviolet (FUV). This spectral range is dominated by photoelectron excited emissions of O and N₂, thus the airglow measurements provide a measure of the influence of the solar radiation on the Earth's atmosphere as well as an indication of the magnitude of the solar irradiance. In the present work, only the soft X-ray photometers are described, the results from the EUV grating spectrograph are presented in a companion paper (Woods *et al.*, 1998) while results from the other instruments will appear in other publications.

The rocket payload itself is described in more detail in an earlier work (Woods *et al.*, 1994). The Lockheed SPARCS attitude control system (ACS) provides pointing towards the sun to within a few arc seconds accuracy. The solar X-ray photometers are located in the solar instrument section which is evacuated prior to launch.

Both rocket flights occurred near local noon at White Sands Missile Range in New Mexico on 4 October 1993 and 3 November 1994 respectively. Solar $F_{10.7}$ values were 121 and 85 for the two rocket flight 5 respectively. The relevant geophysical conditions for each of the rocket flights are described in Table I. Apogee altitudes of 300 km and 280 km were achieved.

The detectors for the Solar X-ray Photometers (SXPS) are silicon XUV photodiodes which are available commercially and discussed in detail by Korde and Geist

TABLE I
Solar and geophysical conditions for rocket flights

	Launch date	UT	Solar zenith angle	$F_{10.7}^{\dagger}$ cm flux	$F_{10.7}^{\dagger}$ cm flux (81 day ave)
NASA 36.107	4 Oct. 1993	17:45	39.9°	121.5	93.3
NASA 36.124	3 Nov. 1994	18:45	47.2°	85.9	82.4

$F_{10.7}^{\dagger}$ cm fluxes are solar radiances at 10.7 cm and are in units of $10^{-22} \text{ W m}^{-2} \text{ Hz}^{-1}$. These fluxes are used as proxies of solar XUV irradiances and uncertainties for their values are not available.

TABLE II
Photodiode coatings used in rocket flights

Coating	Thickness [†] (nm)	Aperture size [‡] (cm ²)	Flight (yr)
Ti, TiO, SiO ₂	500, 500, 5	0.446	1993
Al, SC, C, SiO ₂	150, 50, 45, 5	0.221	1993, 1994
Al, C, SiO ₂	200, 85, 10	0.198	1993, 1994
Zr, Ti, C, SiO ₂	190, 20, 20, 10, 5	0.178	1994
Ti, TiO, SiO ₂	310, 10, 5	0.178	1994

[†]Coating thickness carry a two-sigma uncertainty of 10% based upon deposition measurement:

[‡]Aperture areas carry a two-sigma uncertainty of less than 2%.

(1987), Korde, Canfield, and Wallis (1983), Korde, Cable, and Canfield (1993), and Canfield *et al.* (1994). Their response at short wavelengths is near the theoretical response for silicon. The sensitivity of an uncoated diode is about 1 electron per photon at 340 nm and increases proportionally at a rate of 1 electron per 3.63 eV of photon energy (Korde and Canfield, 1989). Thus, at 10 nm there are approximately 34 electrons per photon. The sensitivity has been shown to be highly stable for large radiation fluences (Canfield, Kerner, and Korde, 1989). The National Institute of Standards and Technology (NIST) uses these XUV photodiodes as secondary standards in the 5 nm to 254 nm spectral region. These Si XUV photodiodes are similar to those flown previously by Ogawa *et al.* (1990).

The photometer bandpass is determined from thin film filters deposited directly on the photodiode in the wafer form (Canfield *et al.*, 1994). The particular material and thickness in conjunction with the uncoated photodiode response, determine the wavelength region of sensitivity for each photometer. The use of several photome-

ters with different filters yields the desired wavelength coverage. Table II lists the filter materials and thicknesses for each photodiode. A total of six photometers can be flown on the rocket payload; Table II lists only those photometers for which data are analyzed in this work. Oxide layers which grow on the metals are taken into account. Transmission properties of the various metals used in this study are available for modeling (Henke *et al.*, 1982; 1988; Powell *et al.*, 1990).

The electronics for the X-ray photometer are simple and are designed for a large dynamic range. The current from the photodiode is converted to a voltage through an operational amplifier. A voltage to frequency converter then translates this voltage into a system of digital pulses such that the frequency is proportional to the original current. Outside the photometer electronics, in the telemetry section of the rocket, are pulse counters which count the pulse rate which is then transmitted to the ground. This method allows for a larger dynamic range as well as a much smaller susceptibility to noise in the measurements. The range of measurable currents for this electrometer system are 1×10^{-12} A to 2×10^{-8} A producing frequencies of 50 Hz to 1 MHz.

The major difficulty in these measurements is the rejection of intense visible light. There are nearly 10 orders of magnitude more photons in the visible than in the soft X-ray region of the solar spectrum and an uncoated XUV photodiode has significant sensitivity in the visible. The coatings are designed to have sufficient soft X-ray transmission and to have the required level of rejection to visible light. However, deposition of a metal film over the entire area of a photodiode causes a short circuit between the anode and cathode of the photodiode. Therefore, the thin film is deposited on the active area and a mask is used to prevent visible radiation from reaching the uncoated regions. The mask complicates the fabrication process but this technique is still preferable to using thin foil filters. Foils are easily damaged and susceptible to pinholes and thus are not well suited for use in space. The coating and mask combination dramatically reduces the visible light and makes solar soft X-ray measurements possible. For some photodiodes a visible background signal still exists at a lower level and is often due to pinholes from the coating process. In practice, several photodiodes are tested and the best are chosen for flight. Improved deposition techniques and better assembly procedures now yield pinhole-free coatings for these diodes.

While the dark current of the XUV photodiodes is usually negligible (less than 10^{-13} A) compared to solar soft X-ray signals, the visible contribution to the background signal can be significant and must be measured in conjunction with the solar soft X-ray measurements. The background measurement is accomplished in flight by moving magnesium fluoride (MgF_2) windows in front of the photometers for a short time near apogee. The MgF_2 passes UV and visible radiation but not soft X-ray or EUV. Therefore, these filters give the magnitude of background signal that is due to long wavelength radiation and any dark current. A correction must be made as the transmission of MgF_2 is slightly less than 100%. The transmissions

of the filters are measured in the laboratory with a tungsten lamp and are typically about 96% at visible wavelengths.

3. Calibration

Calibration of the photodiodes is performed primarily at the NIST Synchrotron Ultraviolet Radiation Facility (SURF II) and the procedures are described in detail by Canfield (1987). Calibrations are performed there from 5 nm to 50 nm. The only calibrations below 5 nm are done with a Fe-55 radioactive source at 0.21 nm. Thus, the region below 5 nm requires models of the photodiode sensitivity. This use of sensitivity calculations is possible because the sensitivity of the uncoated photodiode is well known (Korde and Canfield, 1989) and absorption coefficients for all the coating materials are found in the literature (Henke *et al.*, 1982, 1988; Powell *et al.*, 1990). An additional constraint is that the material thickness is measured as the material is deposited onto the photodiode. The transmission of each coating material is related to material thickness in the following way:

$$T(\lambda) = e^{-\mu(\lambda)\tau}, \quad (1)$$

where T is the transmission, μ is the absorption coefficient for the material, and τ is the thickness. The product of all the modeled transmission and the uncoated photodiode sensitivity gives the sensitivity of the coated photodiode. The procedure is then to perform a calibration at NIST over as broad a wavelength range as possible. This calibration is compared to a model of the sensitivity based on the material thicknesses. Included in the model are estimates for the thickness of the oxide layer, if any, which grows on most metallic films after deposition. The thin film thicknesses are then adjusted to achieve the best possible match between the modeled and measured sensitivities. The modeled sensitivities are used for the full wavelength range. Figure 1 shows the results of this procedure for the photodiodes presented in this work. The plots can be compared with the plot of the sensitivity of an uncoated photodiode which is also shown. Figure 1 shows the measured calibrations with error bars which represent two sigma uncertainty. These uncertainties are provided by NIST.

4. Data Analysis

Each of the photometers listed in Table II obtained useful data that is analyzed in this work. Note that the photodiode set used on the 1994 flight is nearly identical to the 1993 flight with the addition of a Zr/Ti/C coated photodiode and the replacement of the Ti coated photodiode. Table I lists the conditions for the two rocket flights.

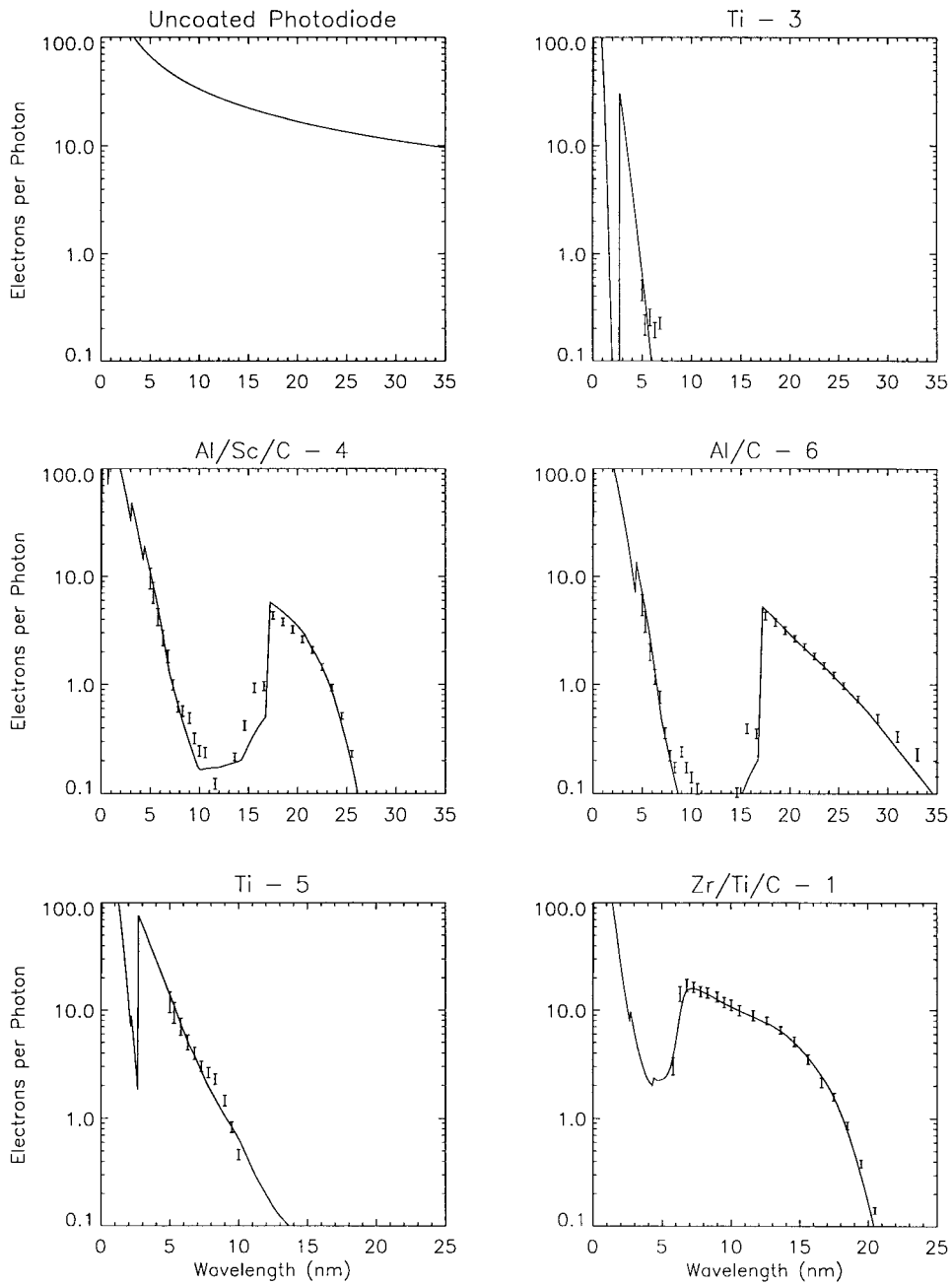


Figure 1. Sensitivity of the coated photodiodes flown on the 1993 and 1994 rocket flights. A model calculation of an uncoated photodiode with no oxide layers is shown for comparison. Uncertainties are discussed in the text.

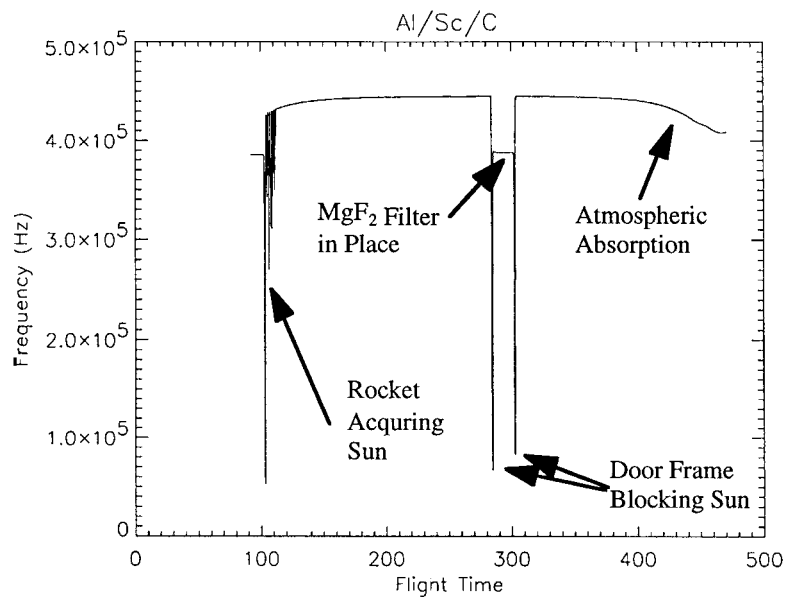


Figure 2. Typical flight profile for a solar X-ray photometer; the Al/Sc/C coated photodiode flown on 3 November 1994 is shown. The period of lower count rate at apogee is the result of closing the door and placing a MgF₂ filter in front of the photometer.

Figure 2 shows the data for the Al/Sc/C coated photodiode flown on the 1994 flight. Prior to 120 s, the rocket is not pointed precisely toward the Sun and the data appears noisy as the Sun moves in and out of the field of view. Once the Sun is acquired, the signal increases as the payload moves up in the atmosphere. At apogee, the door containing the MgF₂ windows is closed. These windows remove the XUV radiation thus lowering the count rate. The door is then reopened and data is taken during the down leg of the flight. As the rocket travels lower in the atmosphere, the signal decreases due to atmospheric absorption of the XUV radiation.

The analysis of the photometer data begins with the measurements made near apogee. After subtracting the longer wavelength background signal corrected for the MgF₂ window transmission and dividing by the aperture size, the soft X-ray radiation data is in units of ampere per cm². Because the solar irradiance and the sensitivity of the photodiode are wavelength dependent over the instrumental passband, the conversion from current to irradiance units is not straightforward. The approach adopted here for this conversion is to scale a model spectrum so that the spectrum convolved with the photometer's wavelength dependent sensitivity yields the measured soft X-ray current. The SERF 1 model spectrum (Hinteregger, Fukui, and Gilson, 1981) appropriate to the conditions of the rocket flight is used for the initial spectrum.

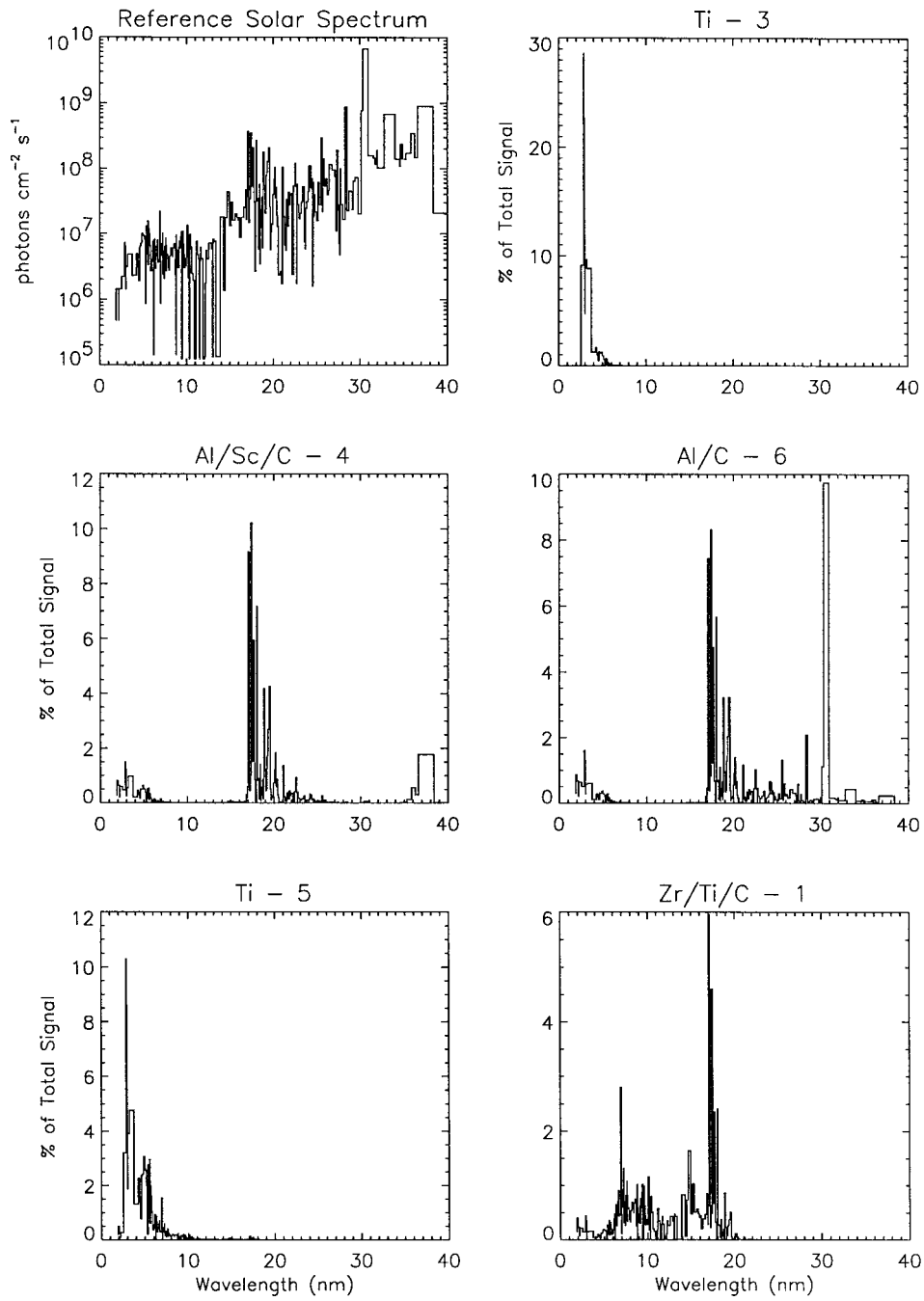


Figure 3. Convolution of SXP sensitivities with reference solar spectrum.

To select the wavelength regions into which the spectrum will be divided, the photometer sensitivity is convolved with the model solar spectrum. The results of such a convolution are given in units of ampere per cm^2 for each wavelength interval. Dividing the result by the total current gives the fraction of current per wavelength interval as shown in Figure 3 as percentages of the total signal. Analysis of Figure 3 shows that the most obvious wavelength intervals are 2 nm to 6 nm (Ti), 6 nm to 17 nm (Zr/Ti/C), and 17 nm to 30 nm (Al/Sc/C, Al/C). A contribution above 30 nm is from the He II 30.4 nm emission in the Al/C coated photometer data. Because this emission was measured with the EUV Grating Spectrograph (EGS) aboard the rocket payload, its measured value is used in this analysis instead of the Al/C photometer result.

The current C_i from photodiode i can be expressed in terms of solar irradiance scaling factors. The equations are of the form

$$C_i = \sum_j A_j \left\{ \sum_{\lambda_j} S_i(\lambda_j) F(\lambda_j) \right\}, \quad (2)$$

where $F(\lambda_j)$ is the model solar irradiance at wavelength λ_j which lies in spectral region j , $S_i(\lambda_j)$ is the sensitivity of diode i at λ_j , and λ_j is the scaling factor for spectral region j . Both F and S_i are in the wavelength bins of the SERF 1 model which are typically approximately 0.1 nm in size. The goal is to solve the set of linear equations for the A_j 's. One solution is to use the Ti coated photometer to solve for the 2 nm to 6 nm scaling factor and then use this result to calculate a 2 nm to 6 nm current in the other photodiodes. This predicted current can then be subtracted from the data yielding a scaling factor for the 6 nm to 17 nm and 17 nm to 30 nm irradiance with the Ti/Zr/C, Al/C, and Al/Sc/C coated photometers. We call this method the back substitution method. A more rigorous method of solving the linear equations with a least squares fit is also used. The similarity in results indicates that either technique is acceptable. The results for the scaling factors obtained from the back substitution method are shown in Table III. This method was used to analyze the measurements from both the 1993 and 1994 rocket flights.

Table III lists the derived scaling factors for the model solar irradiances. The Al/C and Al/Sc/C photodiodes are sensitive in approximately the same wavelength interval and so the average scaling factor derived from their data is presented in Table III. For the 1993 flight, a Ti/Zr/C coated photodiode was not flown; therefore, in the 6 nm to 10 nm region the SERF 1 model is used with a scaling factor of 1.7. This scaling is not a measured value but a reasonable estimate by averaging the other two scaling factors for that date. For both rocket flights, scaling factors of approximately two were required to reproduce the SXP data. The corresponding integrated irradiances from 2 nm to 10 nm and from 5 nm to 57.5 nm are listed in Table IV for comparisons. Above 30 nm, irradiances measured by the EGS are used. Feng, Ogawa, and Judge (1989) tabulate several solar soft X-ray irradiance

TABLE III
Scale factors for solar irradiance model

λ_{\min} (nm)	λ_{\max} (nm)	4 Oct. 1993 scale factors	3 Nov. 1994 scale factors
1.8	6.0	1.35	2.24
6.0	17.0	1.7 [†]	2.26
17.0	30.0	2.06	1.57

[†]This scale factor is not measured but is instead the average of the other two scale factors for that date.

TABLE IV
Solar irradiances from rocket data

λ_{\min} (nm)	λ_{\max} (nm)	4 Oct. 1993 irradiance [†]		3 Nov. 1994 irradiance [†]	
		Measured	Predicted	Measured	Predicted
2	10	1.09 (46.6)	0.93	1.15 (25.3)	0.72
5	57.5	37.9 (24.2)	29.6	25.9 (32.5)	23.2

[†]Irradiances are summed from λ_{\min} to λ_{\max} and in units of 10^9 photons $\text{cm}^{-2} \text{s}^{-1}$. Values in parenthesis are two-sigma uncertainties expressed in percent. These uncertainties are representative of the wavelength range where measurements were made. Predictions are from linear fits using the values found in Feng, Ogawa, and Judge (1989).

measurements and show a range of 0.5×10^9 photons $\text{cm}^{-2} \text{s}^{-1}$ to 1.5×10^9 photons $\text{cm}^{-2} \text{s}^{-1}$ in the wavelength region of 2 nm to 10 nm for $F_{10.7}$ values of 70 to 125. For the same levels of solar activity, Feng, Ogawa, and Judge (1989) show a range of 15×10^9 photons $\text{cm}^{-2} \text{s}^{-1}$ to 40×10^9 photons $\text{cm}^{-2} \text{s}^{-1}$ for the wavelength region 5 nm to 57.5 nm. A linear fit can be performed to the measurements tabulated in Feng, Ogawa, and Judge (1989) to give the following results:

$$I_{2-10} = 0.22 + 0.0059 F_{10.7}, \quad (3a)$$

$$I_{5-57.5} = 7.42 + 0.18 F_{10.7}, \quad (3b)$$

where I_{2-10} and $I_{5-57.5}$ are 10^{-9} times the integrated solar irradiances from 2 nm to 10 nm and 5 nm to 57.5 nm, respectively. Table IV also lists the results of using Equations 3a and 3b to predict the irradiances for the two flights. The predicted and measured irradiances differ by an average of 24%. Given the scatter in the measurements tabulated by Feng, Ogawa, and Judge (1989) and the quoted uncertainties in Table IV, the comparison is considered quite good. This comparison demonstrates that the results reported here are in good agreement with other measurements.

TABLE V
Solar irradiance results

Wavelength bins (nm)		4 October 1993	3 November 1994
λ_{\min}	λ_{\max}	irradiance ($\text{ph cm}^{-2} \text{s}^{-1}$)	irradiance ($\text{ph cm}^{-2} \text{s}^{-1}$)
2.3	3.2	$2.74E + 07$	$2.03E + 07$
3.2	4.4	$1.62E + 07$	$1.13E + 07$
4.4	6	$2.02E + 08$	$2.40E + 08$
6	7	$2.24E + 08$	$2.20E + 08$
7	8	$2.28E + 08$	$2.37E + 08$
8	9	$1.65E + 08$	$1.69E + 08$
9	10	$2.33E + 08$	$2.59E + 08$
10	11	$7.38E + 07$	$8.44E + 07$
11	12	$5.71E + 07$	$6.67E + 07$
12	13	$4.18E + 07$	$4.91E + 07$
13	14	$2.84E + 07$	$3.31E + 07$
14	15	$1.36E + 07$	$1.42E + 08$
15	16	$1.94E + 08$	$1.62E + 08$
16	17	$3.32E + 08$	$3.78E + 08$
17	18	$2.27E + 09$	$1.42E + 09$
18	19	$1.39E + 09$	$7.61E + 08$
19	20	$1.36E + 09$	$6.34E + 08$
20	21	$7.13E + 08$	$2.86E + 08$
21	22	$5.21E + 08$	$1.84E + 08$
22	23	$8.22E + 08$	$4.51E + 08$
23	24	$4.53E + 08$	$2.61E + 08$
24	25	$1.08E + 09$	$5.87E + 08$
25	26	$1.96E + 09$	$1.10E + 09$
26	27	$5.57E + 08$	$2.05E + 08$
27	28	$1.26E + 09$	$1.08E + 09$
28	29	$1.83E + 09$	$1.18E + 09$
29	30	$2.94E + 09$	$1.76E + 09$
30	31	$6.89E + 09$	$4.35E + 09$

The scaling factors determined above can be applied to the SERF 1 model spectrum to yield a solar spectrum representative of the measurements. For the tabulation, the scaled solar spectrum is reported in bin sizes of approximately 1 nm. The results of this process are contained in Table V.

Uncertainty in the soft X-ray measurements comes from several sources. Detector calibration uncertainties are obtained from NIST and included in the total uncertainty calculation. Another source of uncertainty is the detector counting statistics and calibration constants from counts to current, but both are 1% or less. Because calibrations are made at the center of the photodiode, there is an uncertainty in assuming uniform sensitivity across the active area. Although this can only be quantified by a detailed mapping of the active area, an estimate of the two sigma total uncertainty is 20% when detector maps are unavailable. This value is arrived at by analysis of 1993 flight data from the Al/C and Al/Se/C photodiodes, which are sensitive in nearly the same wavelength regions. A two sigma uncertainty of 20% accounts for differences in absolute irradiances derived from these two photodiodes. This uncertainty also includes the application of model sensitivities to wavelength regions where no calibrations are made. The final uncertainties for each measurement are reported in Table IV.

5. Conclusions

We have described measurements of the solar irradiance from 2 nm to 30 nm at times of low to moderate solar activity. An analysis of results from these photometers shows that the appropriate SERF 1 model solar spectrum must be scaled by approximately a factor of two in this wavelength region to achieve agreement between modeled and measured photodiode currents. This result is in agreement with the measurements compiled by Feng, Ogawa, and Judge (1989).

These Si photodiodes with thin film coatings have been proven effective for measuring solar soft X-ray irradiance. Currently there are plans for additional rocket flights of these soft X-ray photometers as well as satellite measurements. We anticipate improvement in the following areas. First, we hope for extended wavelength coverage for the calibrations. A monochromator has been developed for use in the 2 nm to 122 nm range. This monochromator is fitted with an uncoated soft X-ray photodiode as a standard reference detector and uses the SURF beam as a calibration source. This system will have the additional ability to make calibrations at different points on the active area of the photodiode, allowing quantification of coating uniformity. A second area of concentration will be in the reduction of the background signal. Further developments in both masking and the deposition process have already yielded photodiodes with reduced sensitivity to visible radiation. This will result in a higher signal to noise ratio in the data.

Future applications of these photometers include flights on the NASA Thermosphere Ionosphere Mesosphere Energetics and Dynamics (TIMED) satellite, the Student Nitric Oxide Explorer (SNOE), and the German EUV-PHOKAS satellite experiment. SNOE was launched in February 1998. TIMED will be launched in the May of 2000 and will make measurements for at least two years. The techniques used for these two missions are identical to those described here.

Acknowledgements

This research was supported by NASA grant S-09936-F. We thank the SURF II group at NIST for assisting in the photodiode photometric calibrations. We are extremely grateful to the engineering and technical staff at LASP, especially Greg Ucker, Ray Wrigley, Rick Kohnert, and Erica Rodgers. We also thank the NASA Wallops Flight Facility and the WSMR Lockheed personnel for their cooperation and excellent support of this rocket program.

Data Sources

Hinteregger, Fukui, and Gilson (1981) established a solar minimum reference spectrum referred to as SC No. 21REFW. This reference spectrum can be obtained from the National Geophysical Data Center. The data file as well as the results reported in this work and links to other solar data sources can be found at the following Internet address:

<http://lasp.colorado.edu/rocket/rocket-home.html>.

References

- Barth, C. A., Tobiska, W. K., Siskind, D. E., and Cleary, D. D.: 1988, *Geophys. Res. Letters* **15**, 92.
- Buansanto, M. J., Solomon, S. C., and Tobiska, W. K.: 1992, *J. Geophys. Res.* **7**, 10513.
- Canfield, L. R.: 1987, *Applied Optics* **6**, 3831.
- Canfield, L. R., Kerner, J., and Korde, R.: 1989, *Applied Optics* **8**, 3940.
- Canfield, L. R., Vest, R., Woods, T. N., and Korde R.: 1994, *Proc. of SPIE* **2282**, 31.
- Feng, W., Ogawa H. S., and Judge, D. L.: 1989, *J. Geophys. Res.* **4**, 9125.
- Henke, B. L., Lee P., Tanaka, T. J., Shimabukuro, R. L., and Fujikawa, B. K.: 1982, *At. Data Nucl. Data Tables* **27**, 1.
- Henke, B. L., Davis, J. C., Gullikson, E. M., and Perera, R. C.: 1988, *Lawrence Berkeley Laboratory Report LBL-26259*.
- Hinteregger, H. E., Fukui, K., and Gilson, G. R.: 1981, *Geophys. Res. Letters* **8**, 1147.
- Korde, R. and Canfield, L. R.: 1989, *Proc. SPIE* **1140**, 126.
- Korde, R. and Geist, J.: 1987, *Appl. Optics* **26**, 5284.
- Korde, R., Cable, J. S., and Canfield, L. R.: 1993, *IEEE Trans. Nucl. Sci.* **40**, 1655.
- Korde, R., Canfield, L. R., and Wallis, B.: 1988, *Proc. SPIE* **932**, 153.
- Kreplin, R. W.: 1970, *Ann. Geophys.* **26**, 567.
- Kreplin, R. W. and Horan, D. M.: 1992, in R. F. Donnelly (ed.) *Proceedings of the Workshop on the Solar Electromagnetic Radiation Study for Solar Cycle* **22**, 405.
- Lean, J.: 1987, *J. Geophys. Res.* **92**, 839.
- Lean, J.: 1990, *J. Geophys. Res.* **95**, 11933.
- Manson, J. E.: 1976, *J. Geophys. Res.* **81**, 1629.
- Ogawa, H. S., Canfield, L. R., McCullin, D., and Judge, D. L.: 1990, *J. Geophys. Res.* **95**, 4291.
- Powell, F. R., Vedder, P. W., Lindblom J. F., and Powell, S. F.: 1990, *SPIE* **26**, 614.

- Richards, P. G. and Torr, D. G.: 1984, *J. Geophys. Res.* **89**, 5625.
- Richards, P. G. and Torr, D. G.: 1985, *J. Geophys. Res.* **90**, 2877.
- Richards, P. G., Fennelly J. A., and Torr, D. G.: 1994a, *J. Geophys. Res.* **99**, 8981.
- Richards, P. G., Fennelly, J. A., and Torr D. G.: 1994b, *J. Geophys. Res.* **99**, 13283.
- Siskind, D. E., Barth, C. A., and Cleary, D. D.: 1990, *J. Geophys. Res.* **95**, 4311.
- Timothy, A. F. and Timothy, J. G.: 1970, *J. Geophys. Res.* **75**, 6950.
- Tobiska, W. K.: 1991, *J. Atmos. Terr. Phys.* **53**, 1005.
- Tobiska, W. K. and Barth, C. A.: 1990, *J. Geophys. Res.* **95**, 8243.
- Torr, M. R., Torr, D. G.: 1985, *J. Geophys. Res.* **90**, 6675.
- Torr, M. R., Torr, D. G., Ong, R. A., and Hinteregger, H. E.: 1979, *Geophys. Res. Letters* **6**, 771.
- Woods, T. N. and Rottman, G. J.: 1990, *J. Geophys. Res.* **95**, 6227.
- Woods, T. N., Rottman, G. J., Bailey, S. M., and Solomon, S. C.: 1994, *Optical Eng.* **33**, 438.
- Woods, T. N., Bailey, S. M., Rottman, G. J., Worden, J. R., and Solomon, S. C.: 1998, *Solar Phys.* **122**, 133.